Cell Reports Medicine, Volume *5*

Supplemental information

Proteo-metabolomics and patient tumor slice experiments point to amino acid centrality for rewired mitochondria in fibrolamellar carcinoma

Donald Long Jr., Marina Chan, Mingqi Han, Zeal Kamdar, Rosanna K. Ma, Pei-Yin Tsai, Adam B. Francisco, Joeva Barrow, David B. Shackelford, Mark Yarchoan, Matthew J. McBride, Lukas M. Orre, Nathaniel M. Vacanti, Taranjit S. Gujral, and Praveen Sethupathy

Figure S1

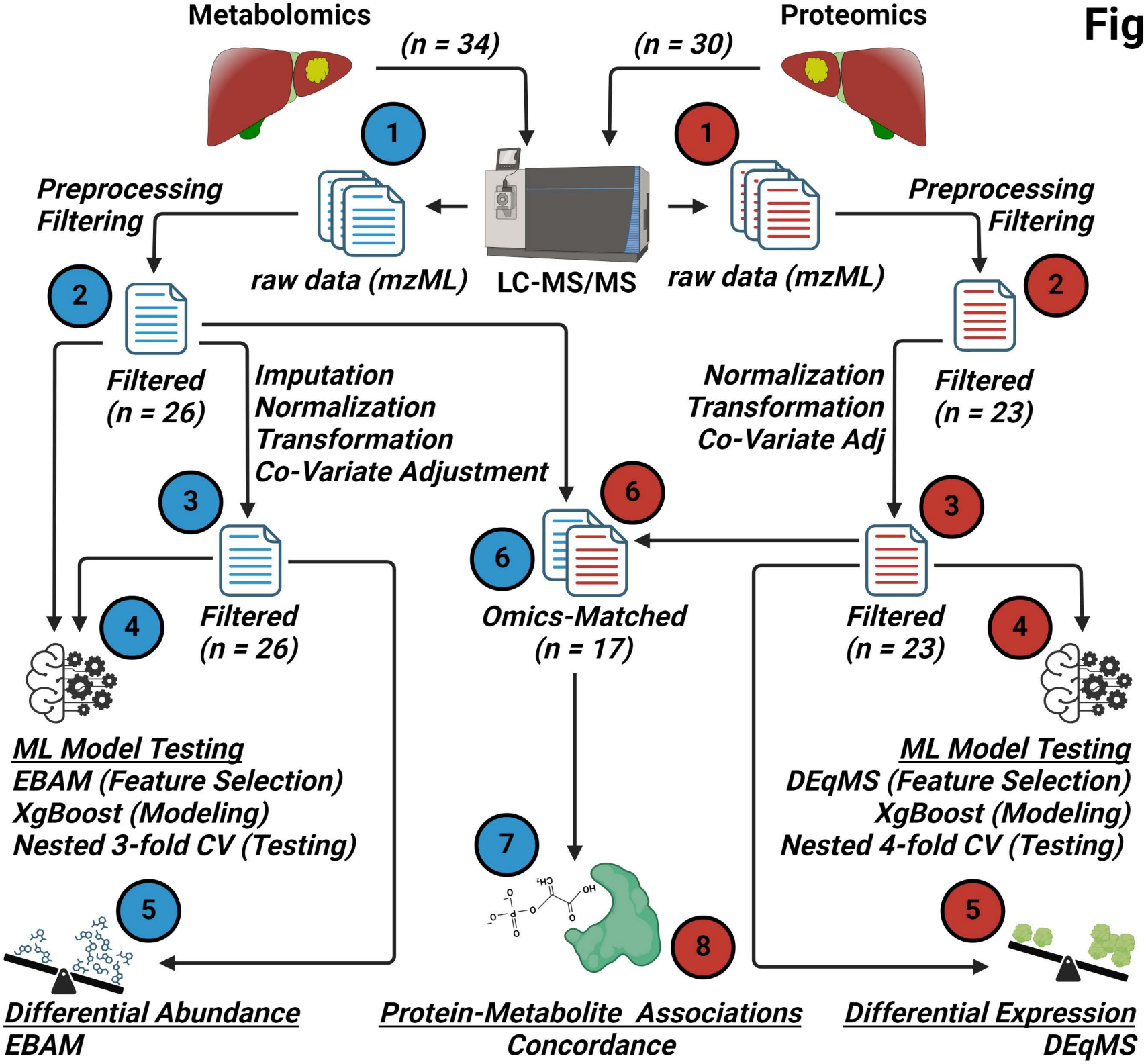
Metabolomics
(n = 34)
Proteomics
(n = 30)
1
1
Preprocessing
Filtering
raw data (mzML)
LC-MS/MS
raw data (mzML)
Preprocessing
Filtering
2
2
Filtered
(n = 26)
Imputation
Normalization
Transformation
Co-Variate Adjustment
Normalization
Transformation
Co-Variate Adj
Filtered
(n = 23)
3
6
6
3
Filtered
(n = 26)
Omics-Matched
(n = 17)
Filtered
(n = 23)
4
4
ML Model Testing
EBAM (Feature Selection)
XgBoost (Modeling)
Nested 3-fold CV (Testing)
ML Model Testing
DEqMS (Feature Selection)
XgBoost (Modeling)
Nested 4-fold CV (Testing)
7
5
8
5
Differential Abundance
EBAM
Protein-Metabolite Associations
Concordance
Differential Expression
DEqMS

Figure S1. Workflow diagram. Schematic of proteomic and metabolomic workflow. LC MS/MS = Liquid Chromatography Mass Spectrometry/Mass Spectrometry; ML = Machine Learning; DEqMS = Differential Expression of quantitative Mass Spectrometry ; XgBoost = Extreme Gradient Boost; CV = Cross-Validation; Adj = Adjusted; EBAM = Empirical Bayes Analysis of Microarrays. Omics-matched refers to patient samples that were present in both the proteomic and metabolomic datasets. **Related to STAR Methods**.

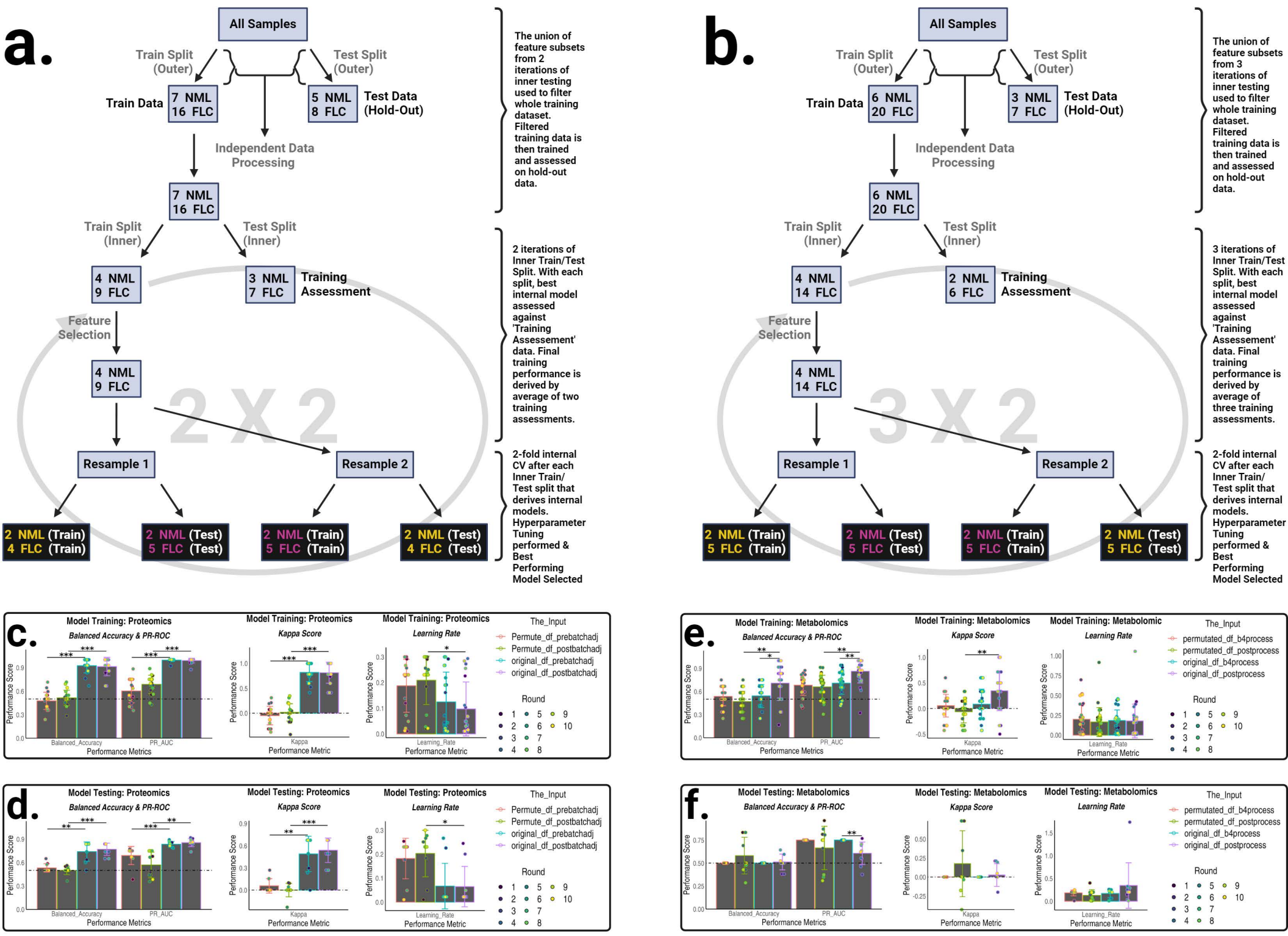
a.
All Samples
Train Split (Outer)
Test Split (Outer)
Train Data
7 NML 16 FLC
5 NML 8 FLC
Test Data (Hold-Out)
Independent Data Processing
7 NML 16 FLC
Train Split (Inner)
Test Split (Inner)
4 NML 9 FLC
3 NML 7 FLC
Training Assessment
Feature Selection
4 NML 9 FLC
2 X 2
Resample 1
Resample 2
2 NML (Train) 4 FLC (Train)
2 NML (Test) 5 FLC (Test)
2 NML (Train) 5 FLC (Train)
2 NML (Test) 4 FLC (Test)
The union of feature subsets from 2 iterations of inner testing used to filter whole training dataset. Filtered training data is then trained and assessed on hold-out data.
2 iterations of Inner Train/Test Split. With each split, best internal model assessed against 'Training Assessement' data. Final training performance is derived by average of two training assessments.
2-fold internal CV after each Inner Train/ Test split that derives internal models. Hyperparameter Tuning performed & Best Performing Model Selected
b.
All Samples
Train Split (Outer)
Test Split (Outer)
Train Data
6 NML 20 FLC
3 NML 7 FLC
Test Data (Hold-Out)
Independent Data Processing
6 NML 20 FLC
Train Split (Inner)
Test Split (Inner)
4 NML 14 FLC
2 NML 6 FLC
Training Assessment
Feature Selection
4 NML 14 FLC
3 X 2
Resample 1
Resample 2
2 NML (Train) 5 FLC (Train)
2 NML (Test) 5 FLC (Test)
2 NML (Train) 5 FLC (Train)
2 NML (Test) 5 FLC (Test)
The union of feature subsets from 3 iterations of inner testing used to filter whole training dataset. Filtered training data is then trained and assessed on hold-out data.
3 iterations of Inner Train/Test Split. With each split, best internal model assessed against 'Training Assessement' data. Final training performance is derived by average of three training assessments.
2-fold internal CV after each Inner Train/ Test split that derives internal models. Hyperparameter Tuning performed & Best Performing Model Selected
c.
Model Training: Proteomics
Balanced Accuracy & PR-ROC
Kappa Score
Learning Rate
Performance Score
Balanced_Accuracy
PR_AUC
Kappa
Learning_Rate
Performance Metrics
Performance Metric
The_Input
Permute_df_prebatchadj
Permute_df_postbatchadj
original_df_prebatchadj
original_df_postbatchadj
Round
1 2 3 4 5 6 7 8 9 10
e.
Model Training: Metabolomics
Balanced Accuracy & PR-ROC
Kappa Score
Learning Rate
Performance Score
Balanced_Accuracy
PR_AUC
Kappa
Learning_Rate
Performance Metrics
Performance Metric
The_Input
permutated_df_b4process
permutated_df_postprocess
original_df_b4process
original_df_postprocess
Round
1 2 3 4 5 6 7 8 9 10
d.
Model Testing: Proteomics
Balanced Accuracy & PR-ROC
Kappa Score
Learning Rate
Performance Score
Balanced_Accuracy
PR_AUC
Kappa
Learning_Rate
Performance Metrics
Performance Metric
The_Input
Permute_df_prebatchadj
Permute_df_postbatchadj
original_df_prebatchadj
original_df_postbatchadj
Round
1 2 3 4 5 6 7 8 9 10
f.
Model Testing: Metabolomics
Balanced Accuracy & PR-ROC
Kappa Score
Learning Rate
Performance Score
Balanced_Accuracy
PR_AUC
Kappa
Learning_Rate
Performance Metrics
Performance Metric
The_Input
permutated_df_b4process
permutated_df_postprocess
original_df_b4process
original_df_postprocess
Round
1 2 3 4 5 6 7 8 9 10

Figure S2

Figure S2. Machine learning using omics datasets performed significantly better than noise at tumor classification. Schematics that depict core principles of nested cross-validation for **(a)** proteomics and **(b)** metabolomics. Total samples for ($n_{proteomics}$ = 36;$n_{metabolomics}$ = 36) were split into a training set ($n_{proteomics}$ = 23 and $n_{metabolomics}$ = 26 samples that were used for analyses involving machine learning & beyond) and a hold-out set ($n_{proteomics}$ = 13 and $n_{metabolomics}$ = 10 additional, independent samples. These samples were used exclusively for machine learning). The data from the training and hold-out sets were processed independently, thereby minimizing data leakage. Training data went through two iterations of inner-loop train ($n_{proteomics}$ = 13 and $n_{metabolomics}$ = 18)/test ($n_{proteomics}$ =10 and $n_{metabolomics}$ = 8) stratified splitting. With each iteration, the inner training (IT) data was subsetted for the most relevant features using a PCA-based method (see Methods). The subsetted IT data was subsequently used for stratified 2-fold,3-repeat cross validation (CV) where each fold (or resample) contained at least **(a)** six (n_{NML} = 2; $n_{FLC} \geq 4$) or **(b)** nine (n_{NML} = 2; n_{FLC} = 7) samples within each partition for training and testing. **(a,b)** Hyperparameter tuning was incorporated into the 2-fold,3-repeat CV. With each iteration, the best model from the inner training was assessed for performance against the inner test data. Overall evaluation of training performance was attained by averaging the **(a)** two or **(b)** three training assessments from the **(a)** two or **(b)** three iterations of inner training. The union of the feature subsets from the **(a)** two or **(b)** three iterations was used to subset the whole training dataset, and 2-fold,3-repeat CV with hyperparameter tuning was performed. A final evaluation was executed by assessing the performance of the trained model against the hold-out set. Bar plots displaying performance metrics generated from machine learning (ML) pipeline (see Methods for further details) using **(c,d)** proteomic and **(e,f)** metabolomic data as input. Performance metrics are associated with the **(c,e)** training phase or **(d,f)** testing phase of the machine learning algorithm. **(c-f)** Dot dash line represents threshold at which the model performs no better than random chance. Mann Whitney used for statistical analysis—*BH-adj pval < 0.05; **BH-adj pval < 0.01; *** BH-adj pval < 0.001. Permute_df_prebatchadj = permutated proteomics dataset without batch adjustment; Permute_df_postbatchadj = Batch-adjusted, permutated proteomics dataset; original_df_prebatchadj = original proteomics dataset without batch adjustment; original_df_postbatchadj = original proteomics dataset with batch adjustment; permutated_df_b4process = permutated metabolomics dataset prior to processing (prior to normalization, transformation, or co-variate adjustment); permutated_df_postprocess = permutated metabolomics dataset that has been processed; original_df_b4process = original metabolomics dataset prior to processing (prior to normalization, transformation, or co-variate adjustment); original_df_postprocess = original metabolomics dataset that has been processed; PR_AUC = precision-recall area under the curve; Round represents consecutive rounds of full pipeline (nested cross-validation) execution. For learning rate, lower values indicate better learning. **Related to STAR Methods**.

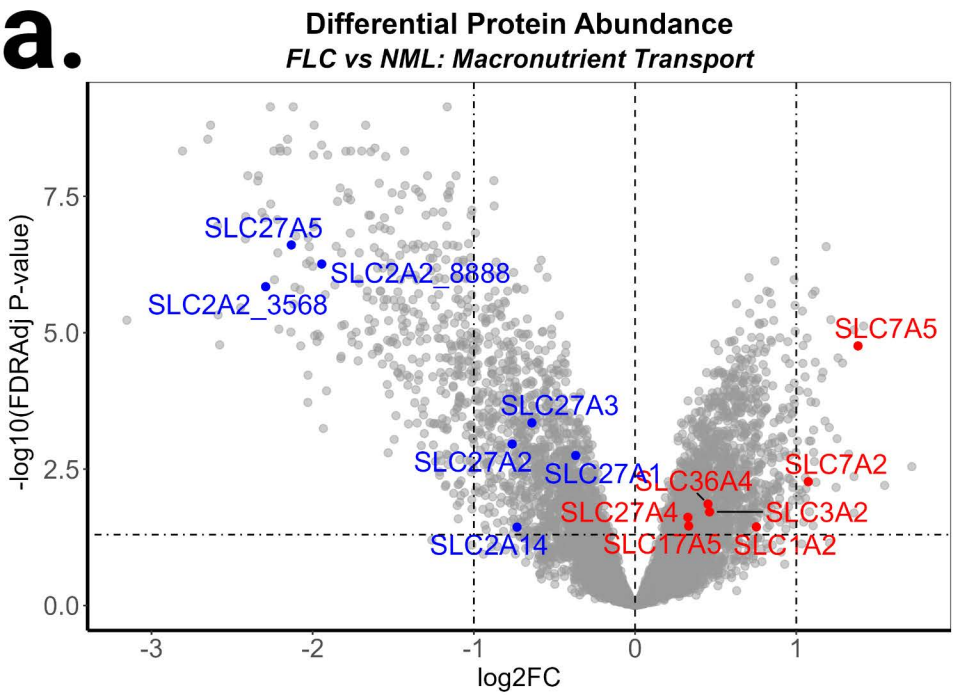
a.
Differential Protein Abundance
FLC vs NML: Macronutrient Transport
-log10(FDRAdj P-value)
log2FC
SLC27A5
SLC2A2_8888
SLC2A2_3568
SLC7A5
SLC27A3
SLC27A2
SLC27A1
SLC36A4
SLC7A2
SLC27A4
SLC3A2
SLC2A14
SLC17A5
SLC1A2

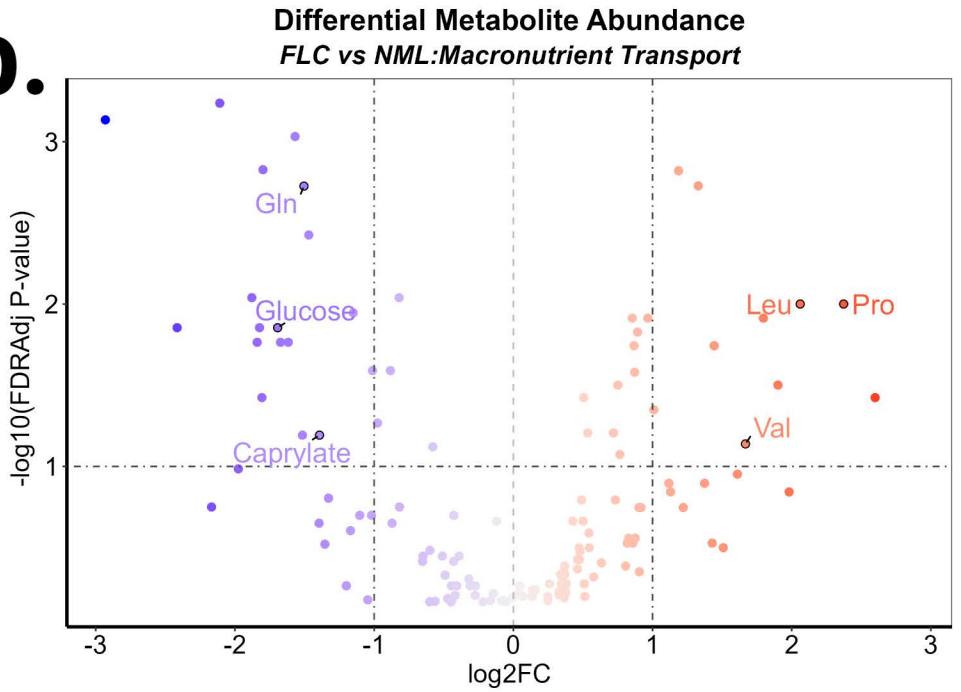
b.
Differential Metabolite Abundance
FLC vs NML:Macronutrient Transport
-log10(FDRAdj P-value)
log2FC
Gln
Glucose
Leu
Pro
Val
Caprylate

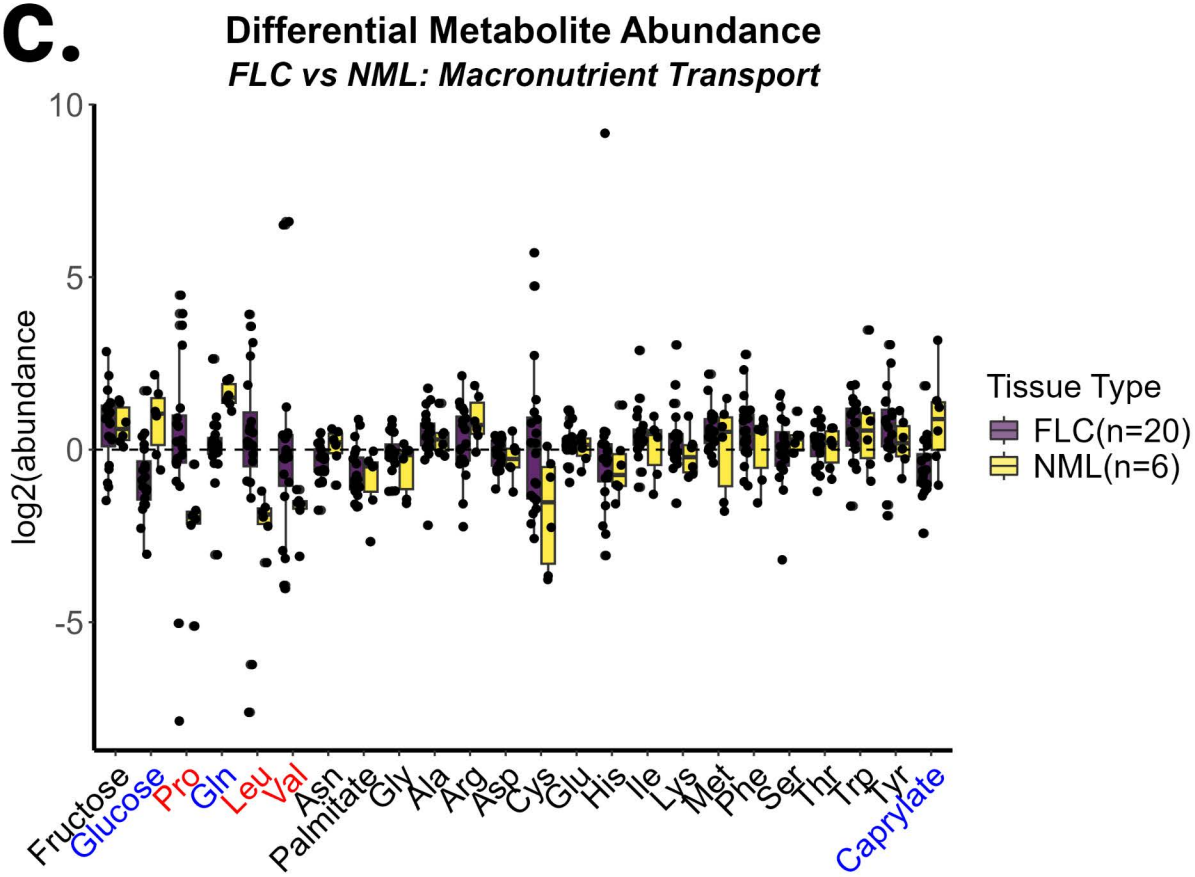
c.
Differential Metabolite Abundance
FLC vs NML: Macronutrient Transport
log2(abundance
Tissue Type
FLC(n=20)
NML(n=6)
Fructose
Glucose
Pro
Gln
Leu
Val
Asn
Palmitate
Gly
Ala
Arg
Asp
Cys
Glu
His
Ile
Lys
Met
Phe
Ser
Thr
Trp
Tyr
Caprylate

Figure S3

Figure S3. Macronutrient profile in FLC. Volcano plots and box plot show abundance of **(a)** proteins and **(b,c)** metabolites. **(a,b)** Highlighted datapoints and colored labels denote down-regulated (blue) or up-regulated (red) **(a)** proteins (fdr-adj $p < 0.05$; $n = 23$ samples) or **(b,c)** metabolites (fdr-adj $p < 0.1$; $n = 26$ samples). **Related to Figure 1**.

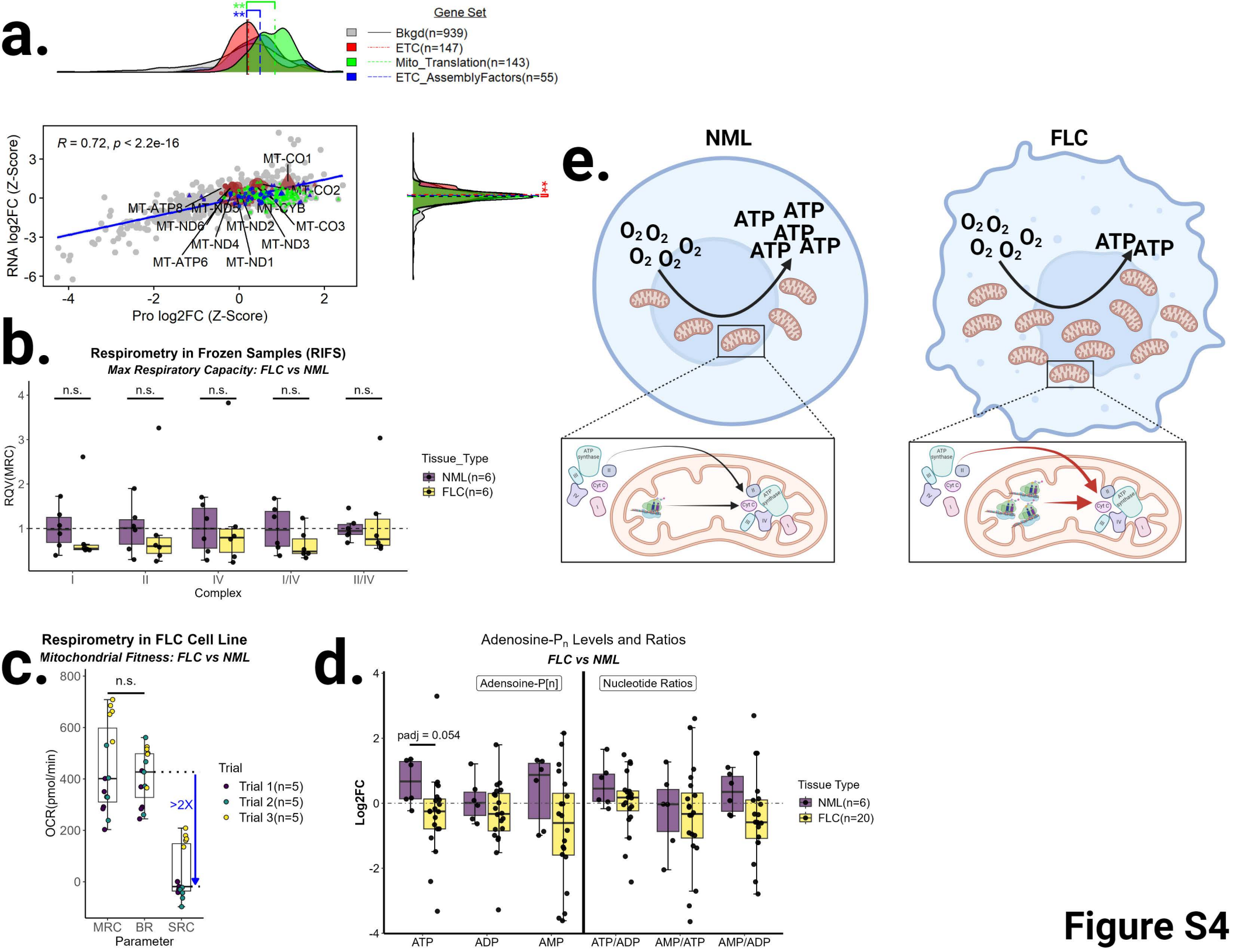
a.
Gene Set
Bkgd(n=939)
ETC(n=147)
Mito_Translation(n=143)
ETC_AssemblyFactors(n=55)
R = 0.72, p < 2.2e-16
RNA log2FC (Z-Score)
Pro log2FC (Z-Score)
MT-CO1
MT-CO2
MT-ATP8
MT-ND5
MT-CYB
MT-ND6
MT-ND2
MT-CO3
MT-ND4
MT-ND3
MT-ATP6
MT-ND1
b.
Respirometry in Frozen Samples (RIFS)
Max Respiratory Capacity: FLC vs NML
RQV(MRC)
n.s.
I
II
IV
I/IV
II/IV
Complex
Tissue_Type
NML(n=6)
FLC(n=6)
e.
NML
FLC
ATP
c.
Respirometry in FLC Cell Line
Mitochondrial Fitness: FLC vs NML
OCR(pmol/min)
n.s.
>2X
MRC
BR
SRC
Parameter
Trial
Trial 1(n=5)
Trial 2(n=5)
Trial 3(n=5)
d.
Adenosine-Pn Levels and Ratios
FLC vs NML
Adensoine-P[n]
Nucleotide Ratios
padj = 0.054
Log2FC
ATP
ADP
AMP
ATP/ADP
AMP/ATP
AMP/ADP
Tissue Type
NML(n=6)
FLC(n=20)

Figure S4

Figure S4. Proteo-transcriptomic signature and functional assessment of mitochondrial respiration suggests ETC dysfunction. (a) Comparison of log2FCs (z-scaled) at the protein (x-axis; n = 23 samples) and RNA (y-axis; n = 27 samples) level. Density plots represent the distribution of the log2FCs. Lines = median. Labeled datapoints = mitochondrially translated ETC subunits. Gene sets were compared to bkgd using Mann Whitney (**fdr- adj p < 0.01). Bkgd = Background. MitoCarta3.0 was used to identify gene sets. **(b)** MRC of ETC complexes in matched, frozen patient tissue per gram of protein (n = 6 samples per tissue type). Per gram protein is representative of collective MRC. RQV = relative quantitative value. **(c)** Assessment of MRC, SRC (spare respiratory capacity), and basal respiration (BR) of mitochondria in FLC cell line (n = 5 per trial). OCR = Oxygen consumption rate. **(d)** Abundance levels and ratios of ATP, ADP, and AMP from frozen patient tumor (FLC, n=20) and non-malignant liver (NML, n=6) tissue. **(e)** Descriptive model depicting dysfunction of mitochondrial respiration in FLC. **Related to Figure 3**.

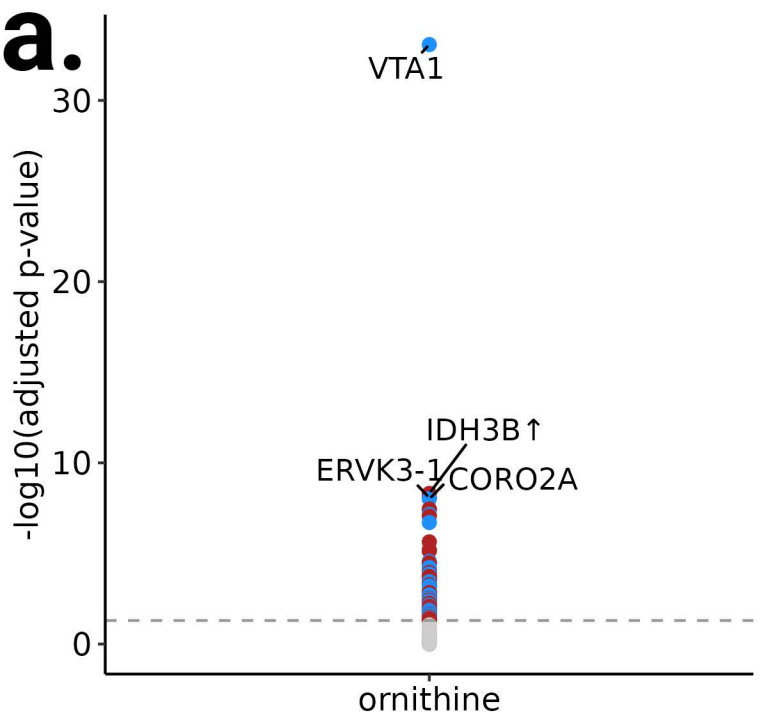

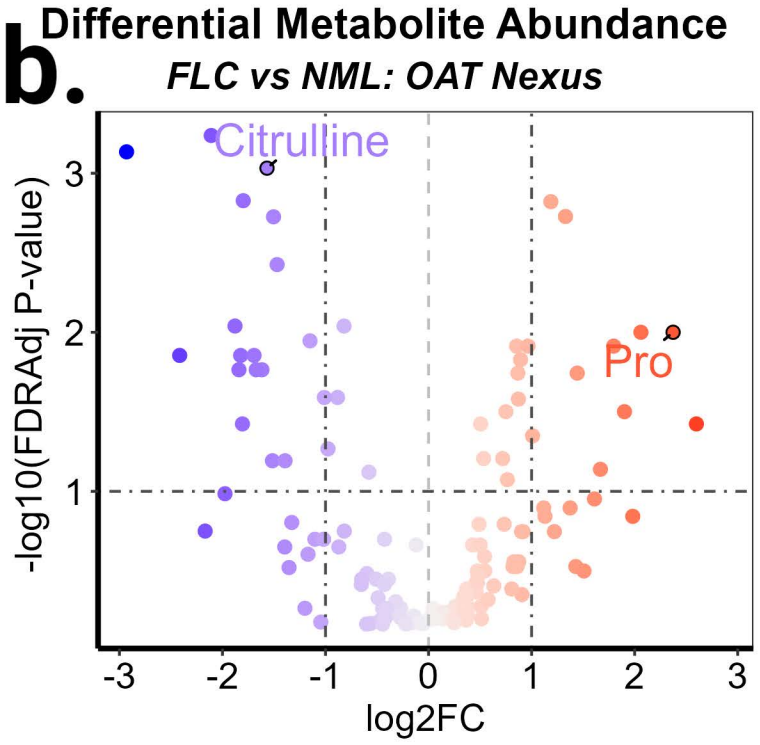

c. **Clinical Features & Outcomes of Patients with FLC-Induced Hyperammonemia**

	Cases(Proportion)	Cases(Percentage)
Suspected OTC Deficiency	11/18	61.1%
Confirmed OTC mutation	0/11	0%
Positive Reponse to Arg Supplementation	7/9	77.8%
Unreposnsive to Arg Supplementation	2/9	22.2%

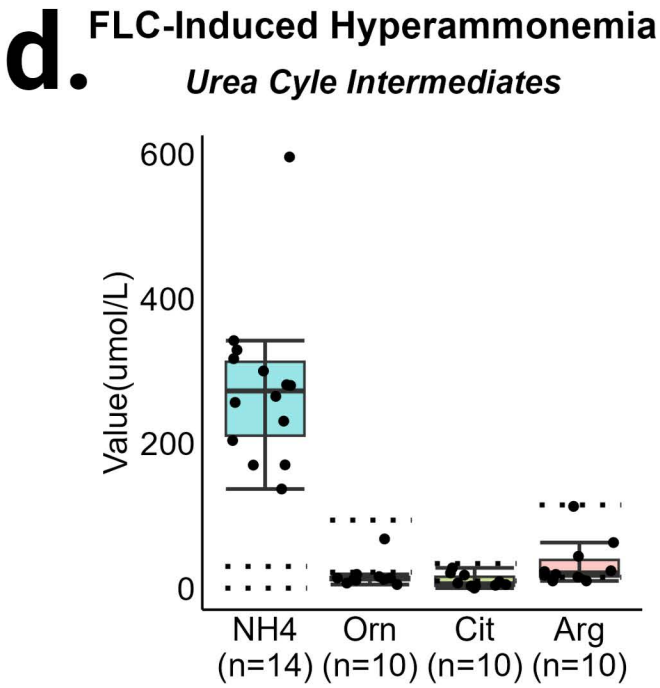

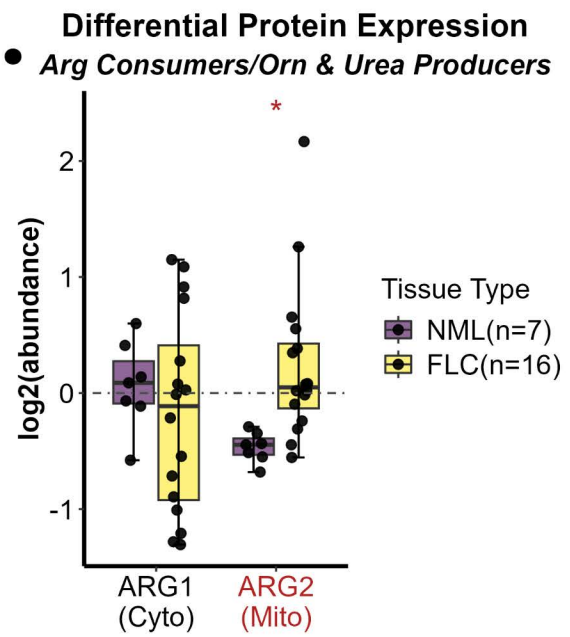

Figure S5

Figure S5. Rewiring of the TCA cycle is associated with urea cycle defects in FLC. (a) Concordance (n = 17 omics-matched sample pairs, 13 of which are FLC) between abundance of proteins (datapoints) and ornithine. Colored datapoints denote protein-metabolite pairs that are significantly (-log10(fdr-adj p) > 1.3) concordant (red) or discordant (blue) in FLC. Labeled datapoints represent the top four associations. Arrows adjacent to labels denote direction of significant alterations in the abundance of proteins (datapoints; fdr-adj $p < 0.05$) in FLC (n = 16 samples) compared to NML (n = 7 samples). Gray datapoints = no significance. **(b)** Volcano plot highlighting the abundance of key metabolites associated with OAT nexus. Highlighted datapoints associated with colored labels denote metabolites that display differential abundance in FLC (n = 20 samples) compared to NML (n = 6 samples). **(c)** Table depicting clinical features and outcomes from our meta-analysis of case studies involving patients with FLC-associated hyperammonemia encephalopathy (HAE). OTC = ornithine transcarbamylase; Arg = arginine. **(d)** Ammonia (serum; n = 14 cases) and amino acid (plasma; n = 10 cases) levels from case studies involving patients with FLC-associated HAE. Area between the dotted lines = reference range. **(e)** Differential protein expression of arginases in FLC (n = 16) compared to NML (n = 7)—*fdr-adj $p < 0.05$. **Related to Figure 6**.

Figure S6

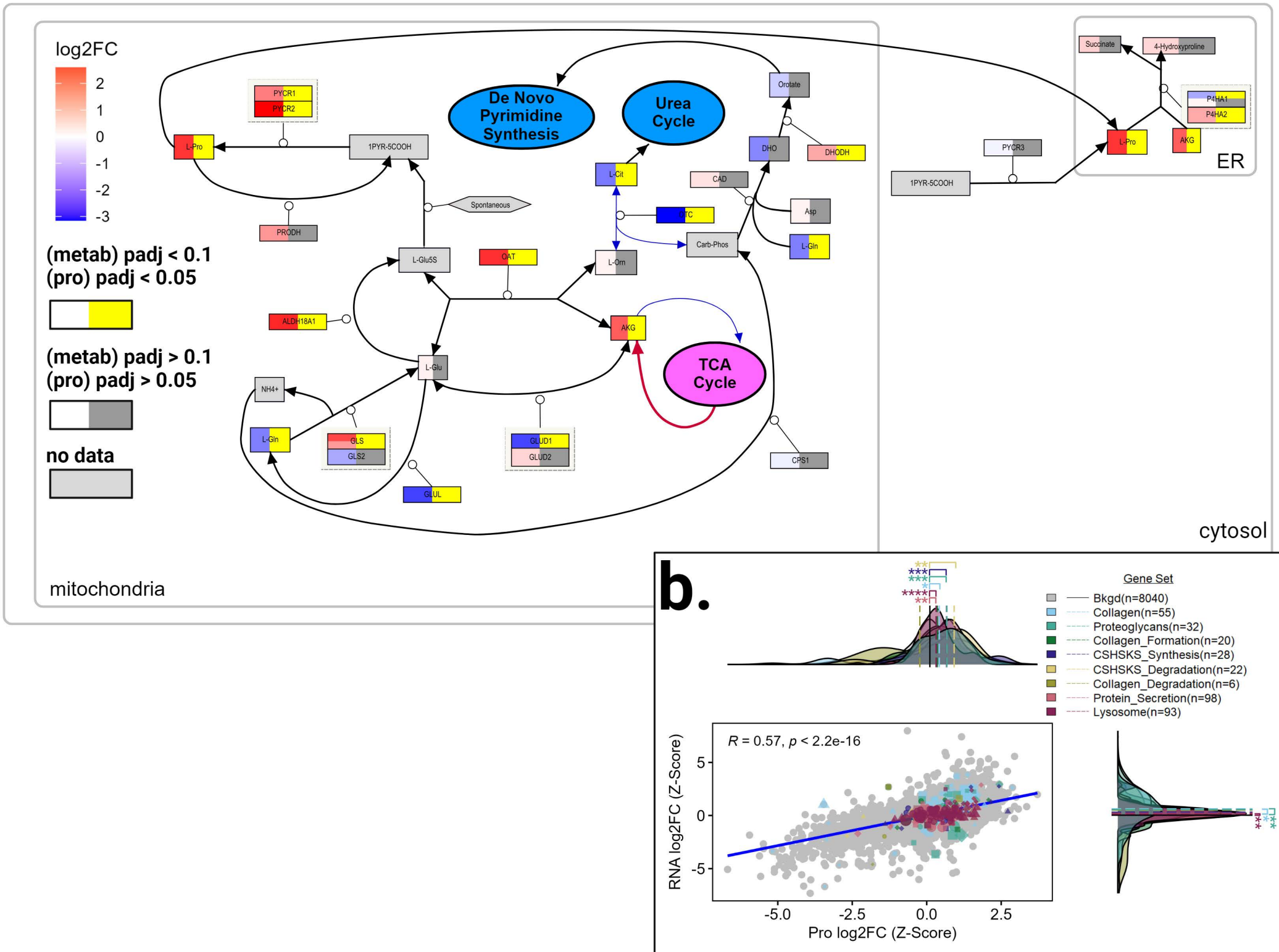
a.
log2FC
2
1
0
-1
-2
-3
(metab) padj < 0.1
(pro) padj < 0.05
(metab) padj > 0.1
(pro) padj > 0.05
no data
mitochondria
cytosol
ER
De Novo Pyrimidine Synthesis
Urea Cycle
TCA Cycle
PYCR1
PYCR2
L-Pro
1PYR-5COOH
PRODH
Spontaneous
L-Glu5S
OAT
ALDH18A1
L-Glu
NH4+
L-Gln
GLS
GLS2
GLUL
GLUD1
GLUD2
CPS1
AKG
L-Orn
L-Cit
OTC
Carb-Phos
CAD
DHO
DHODH
Orotate
Asp
L-Gln
PYCR3
Succinate
4-Hydroxyproline
P4HA1
P4HA2
b.
Gene Set
Bkgd(n=8040)
Collagen(n=55)
Proteoglycans(n=32)
Collagen_Formation(n=20)
CSHSKS_Synthesis(n=28)
CSHSKS_Degradation(n=22)
Collagen_Degradation(n=6)
Protein_Secretion(n=98)
Lysosome(n=93)
R = 0.57, p < 2.2e-16
RNA log2FC (Z-Score)
Pro log2FC (Z-Score)
5
0
-5
-5.0
-2.5
0.0
2.5

Figure S6. Rewired OAT nexus in FLC may be to fuel ECM remodeling. (a) Descriptive model embedded with omics data (proteomics—n = 23 samples; metabolomics—n = 26 samples) depicting OAT nexus in FLC. Left side of each node—gradient red = increasing log2FC (FLC vs NML) and gradient blue = decreasing log2FC; right side of each node—gray = not significant and yellow = significant (proteins—fdr-adj $p < 0.05$; metabolites—fdr-adj $p < 0.1$); nodes associated with edges that have open circles = proteins; nodes associated with edges that have solid arrows = metabolites; ellipses = pathways; red arrow = hypothesized enhancement; blue arrow = hypothesized suppression. **(b)** Comparison of log2FCs (FLC vs. NML; Z-Scaled) at protein (n=23 samples) and RNA (n=27 samples) level for genes that participate in extracellular matrix remodeling. Protein Atlas, Uniprot, and Reactome were used to identify gene sets. Gene sets were compared to bkgd using Mann Whitney test (*FDR adjusted $p < 0.05$; **fdr adjusted $p < 0.01$;***adjusted $p<0.001$;****adjusted $p<0.0001$). Background set (bkgd) is all genes identified in both omics' datasets. For the gene sets (excluding bkgd): circles = genes with no significant log2FCs at either RNA or protein level; diamonds = genes with significant log2FCs at both the RNA and protein level; triangles = genes with significant log2FCs at protein level; squares = genes with significant log2FCs at RNA level; shape size = average gene expression values (from transcriptomic data). **Related to Figure 7.**

Figure S7

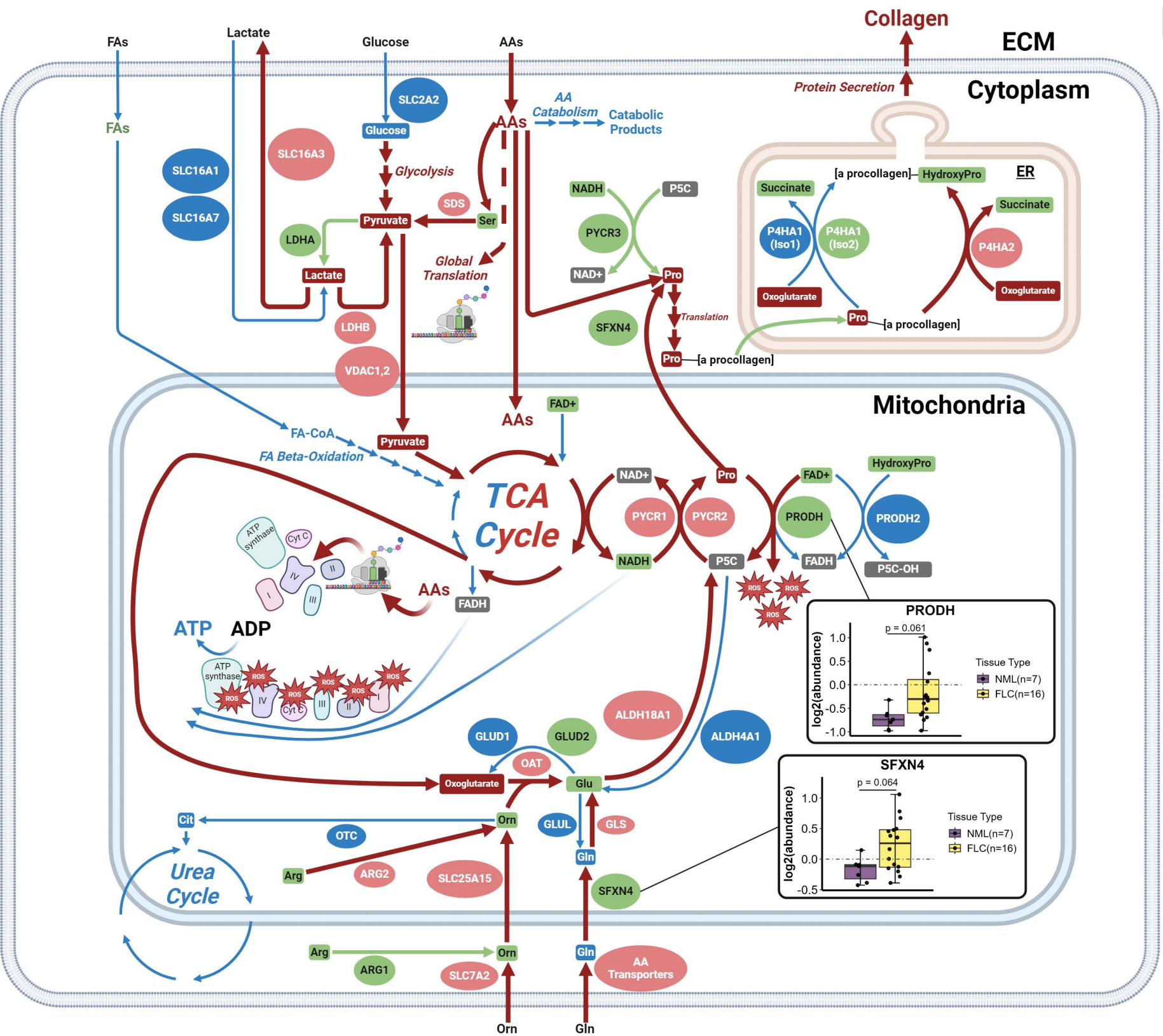
Collagen
ECM
Protein Secretion
Cytoplasm
FAs
Lactate
Glucose
AAs
SLC2A2
AA Catabolism
Catabolic Products
SLC16A3
SLC16A1
SLC16A7
Glycolysis
SDS
Ser
Pyruvate
LDHA
Lactate
LDHB
VDAC1,2
Global Translation
NADH
P5C
PYCR3
NAD+
Pro
Translation
SFXN4
[a procollagen]
ER
Succinate
HydroxyPro
P4HA1 (Iso1)
P4HA1 (Iso2)
P4HA2
Oxoglutarate
Mitochondria
FA-CoA
FA Beta-Oxidation
FAD+
TCA Cycle
NAD+
PYCR1
PYCR2
PRODH
PRODH2
FADH
P5C-OH
ROS
ATP synthase
Cyt C
ATP
ADP
PRODH
p = 0.061
log2(abundance)
Tissue Type
NML(n=7)
FLC(n=16)
ALDH18A1
ALDH4A1
GLUD1
GLUD2
OAT
Oxoglutarate
Glu
Cit
Orn
OTC
GLUL
GLS
Gln
Urea Cycle
Arg
ARG2
SLC25A15
SFXN4
SFXN4
p = 0.064
ARG1
SLC7A2
AA Transporters

Figure S7. Working model of FLC metabolism. Arrow size is directly associated with arrow color. Node size is arbitrary. Red = increase; green = neutral; blue = decrease; gray = no data; elliptical node = protein; square node = metabolite; arrow = reaction or transport; broken arrows = series of reactions; ROS = reactive oxygen species. Sections pertaining to ROS, GLUD, and electron transfer are implications of the model as opposed to direct data. **Related to Figures 1-7**.